Numerical modeling of reinforcement forces in geosynthetic reinforced soil slopes

Houcine Djeffal (houcine.djeffal@yahoo.com)
Ecole Nationale Polytechnique
Smain Belkacemi
École Nationale Polytechnique: Ecole Nationale Polytechnique
Djamalddine Boumezrane
University of the West of Scotland

Research Article

Keywords: Geosynthetics, Reinforced soil slope, Limit equilibrium, Safety factor, Reinforcement force

Posted Date: April 19th, 2021

DOI: https://doi.org/10.21203/rs.3.rs-414771/v1

Manuscript title:

Numerical modeling of reinforcement forces in geosynthetic reinforced soil slopes

Authors: H. Djeffal[1], S. Belkacemi[1], D. Boumezrane[2]

Affiliation:

[1] Civil Engineering Department, Ecole Nationale Polytechnique, 10 Avenue des frères Ouddek, Hassan Badi, BP182-El Harrach, 16200 Alger, Algeria. E-mail: houcine.djeffal@yahoo.com

[2]Engineering Division, University of the West of Scotland. E-mail: Djamalddine.boumezerane@uws.ac.uk

Corresponding author:

H. Djeffal, Civil Engineering Department, Ecole Nationale Polytechnique, 10 Avenue des frères Ouddek, Hassan Badi, BP182-El Harrach, 16200 Alger, Algeria.

E-mail: houcine.djeffal@yahoo.com (*corresponding author*);

Abstract:

Reinforced soil slopes are widely used in civil engineering for slope protection for their vast advantages. The paper reports the details of numerical models used to predict the factors affecting force distribution in the reinforcement layers of reinforced slope-instrumented structures. However, the failure mechanism of reinforced slopes has not been fully studied. The stability analysis of reinforced slopes is conducted in this paper based on the limit equilibrium method. Furthermore, the effects of the target factor of safety and the soil friction angle of the reinforcement layers on the reinforcement force distribution are investigated. The research results indicate that the above parameters have great effects on the maximum reinforcement force and the reinforcement force distribution of the reinforced slope. Based on the analysis of computation results, the reinforcement mechanism is analyzed and the optimum design scheme of the reinforced slope is recommended. The results can be used as a guideline for the determination of the required reinforcement forces.

Keywords: Geosynthetics, Reinforced soil slope, Limit equilibrium, Safety factor, Reinforcement force

1. Introduction

Reinforced slope construction involves the determination of reinforcement spacing and selection of reinforcing materials. The reinforcement sizing is affected by the total force required for slope stabilization and the force distribution in the reinforcement layers along the depth of the reinforced slope (Djeffal and Belkacemi, 2021). Literature indicates different views on the location of maximal reinforcement force and distribution of reinforcement force along slope elevation. Limited researchers have assumed that the distribution of mobilized tension in the geosynthetic layers is highly non-uniform with maximum tension mobilized in the reinforcement layer located near the toe of the slope (Shiwakoti et al., 1999), while some

others assumed that it occurs at the mid-slope height (Zornberg et al., 1998a; Miyata et al., 2018; Salem et al., 2018; Zhang et al., 2018; Allen et al., 2019; Yang et al., 2019). The reinforcement tensile forces distribution in the reinforcement's layers is highly non-uniform along with the slope height. In most of the design problems, it has been assumed that the tension mobilized is minimal in the geosynthetic layer placed at the slope crest and is maximal in the geosynthetic layer installed near the toe of the slope, following a triangular pattern. The assumed distribution of the reinforcement force will have important implications in design, particularly when zones of different reinforcement strength are used along the height of the reinforced slope (Zornberg and Arriaga, 2003).

The interaction coefficient has a significant influence on the form of reinforcement force distribution (Djeffal and Belkacemi, 2020; Shukla et al., 2009; Feng et al. 2018, 2019; Mirzaalimohammadi et al., 2019). In this approach, the choice of the soil-reinforcement interaction coefficient is derived from the choice of structural, geometrical, and mechanical characteristics of the reinforcement. Signified if we want to have a targeted reinforcement force distribution, we have to good select the interaction coefficient.

However, the effects of several factors that may affect the tension distribution of reinforcement layers on the stability of the reinforced slope have not been systematically investigated and are still not clear. In this paper, based on the limit equilibrium theory, the stability analysis of the reinforced slope is conducted with the process developed by Djeffal and Belkacemi in 2020. Furthermore, the effects of the location of reinforcement force with the target safety factor and the critical failure surface are investigated and analyzed based on the analysis of the calculation results.

Djeffal and Belkacemi (2020) developed a procedure to evaluate soil reinforcement forces using common classical limit equilibrium procedures by considering the soil-reinforcement

interaction coefficient effect on reinforcement tension distribution, on mobilization level of reinforcement tensile force and on mobilized level of soil shear strength.

In this work, a parametric study has been carried out on geosynthetic reinforced soil slope using a numerical model of reinforced soil slopes, normalized slope heights were drawn up, based on field data of reinforced slope problem, to figure out the distribution of required tensile force. Reinforcement forces in reinforcement layers are evaluated for the case of uniform safety factor within the reinforced slope.

To study the distribution of reinforcement forces along the depth of reinforced soil slopes, number of simulations of reinforced slopes using the formulation proposed by Djeffal and Belkacemi (2020) were carried out. The factors that may affect the tension distribution in the reinforcement layers were also studied. Based on the results from the numerical models, the reinforcement force distributions in the reinforcement layers in reinforced soil slopes were analyzed by using limit analysis iteratively apply a Modified Bishop Method.

2. Formulation

Djeffal and Belkacemi (2020) determined the required tensile strength redistribution along each reinforcement layer starting from the top layer. The computational approach enables assessment of reinforcement tensile forces at each reinforcement layer and reconsiders the distribution of reinforcement loading along the critical surface. The ultimate outcome of this iterative process is the determination of a new reinforcement tensile forces distribution.

In the formulation proposed by Djeffal and Belkacemi (2020), the phase 1 enables to select the reinforcement tensile force in slope surface, and in the second phase, there will be a redistribution of the reinforcement force by considering the pullout resistance. The implicit steps in the top-down procedure are shown in Fig 1.

In the present paper, we use safety factor FS>1 in all stages (internal and external stability). We also examine the effect of the mobilized reinforcement tension within reinforced soil slope for a different level of factors affecting force distribution in the reinforcement layers.

In the present formulation, mobilized reinforcement tensile resistance is considered as the additional resistance needed to maintain upper layers in equilibrium as a single block. Step by step, starting from the top layer to the bottom, the reinforcement tensile resistances are then determined by considering the mobilized tensile resistance in upper reinforcements as known independently of forces in the lower layers (Djeffal and Belkacemi, 2020).

T_j is the reinforcement tensile force of the j th reinforcement layer expressed in Eq.(1) as :

$$T_j = \left(FS_m M_D - M_R - FS_m \sum_{k=1}^{j-1} T_k H_k \right) / FS_m H_j \quad (1)$$

Where FS_m Safety factor based on moments equilibrium, M_R is the resisting moment developed by the soil strength, M_D is the driving moment due to driving shear forces developed along the failure surface, n is the number of reinforcement layers, and H_j the resulting moment arm of the resulting tensile reinforcement force of the jth reinforcement layers.

The flowchart of the procedure is shown in Fig. 2.

3. Numerical slope model

The numerical model is based on a reported field data from a reinforced soil trial slope developed by Fannin and Hermann (1990), constructed on a competent gravelly sand foundation in Norway. The reinforced soil slope is 4.8 m high, with an inclination of 2:1. Backfill and foundation soil have a unit weight 17 kN/m^3, an internal friction angle of 38° and a cohesion term of 2 kPa. Two different reinforcement sections schemes were used at the site, as shown in Fig. 3, namely section J and N in the original paper.

4. Results and discussion

Results of this parametric study are discussed in the following section. Measured and calculated reinforcement forces in each layer of two sections are shown in figures 4 to 8. These figures compare the force distribution in reinforcement layers of same height and different reinforcement layer spacing.

There are many factors that may affect the tension distribution in the reinforcement layers, such as soil strength parameters, slope geometry, soil-reinforcement interaction and surcharge pressure. In this section, numbers of simulations have been made to study the factors that may affect the location of maximum reinforcement force and its distribution in the reinforcement layers.

4.1. Effect of target safety factor

Required reinforcement forces in reinforcement layers of two sections were obtained by setting the safety factor value (Fs=1.0, 1.1 and 1.2) and varying soil-reinforcement interaction coefficient value, as shown in Fig. 4, 5 and 6.

Soil-reinforcement interaction coefficient was varied in Fig. 4 for different values of the safety factor of reinforced slope (figures a, b and c). Increasing the factor of safety induced a change in, the reinforcement force distribution for section J scheme. Reinforcement force distribution is sensitive to values of soil-reinforcement interaction coefficient. This result agrees with the numerical studies of Xie et al., (2016) and Djeffal and Belkacemi (2020).

Soil-reinforcement interaction coefficient was varied in section N, shown in Fig. 5.As the safety factor of reinforced slope increased in figures a, b and c, the reinforcement force distribution changed and is sensitive to values of soil-reinforcement interaction coefficient. The target safety factor was a good indicator of the reinforcement forces values compared to that measured in the reinforcements for geosynthetic-reinforced slopes built with different

configurations. This result is in agreement with the numerical study of Xie, and al., (2016) and of Djeffal and Belkacemi (2020).

The point, at 0.25 normalized elevation, where the graphs in Fig.4 and Fig. 5 converge to similar values of reinforcement force could reveal details about a change in the mechanism or mode of mobilized soil-reinforcement interaction.

Fig. 6shows the effects of variation of soil-reinforcement interaction coefficient on sum of reinforcement force for different values of safety factor of 1, 1.1 and 1.2.Two sections J and N are shown. The results show that the sums of reinforcement forces are highly affected by the soil-reinforcement interaction coefficient. For the two sections, as the target safety factor value increases, the required reinforcement tensile force increases. Required reinforcement tensile forces are very dependent on the predefined value of the safety factor. This result is in agreement with the numerical study of Tiwari and Samadhiya (2015) and of Chen et al. (2017).

4.2. Effect of soil friction angle

Soil shear strength was varied using friction angle as shown in Fig. 7 and 8, with the safety factor and the soil-reinforcement interaction held constant. Values of interaction coefficient Ci=0.05 give a comparable and similar results to the measured result independently of slope models (Djeffal and Belkacemi, 2020).

The effects of soil internal friction angle, on reinforcement force distribution are shown in Fig. 7 and 8 where we can see increase of reinforcement force with the decrease in soil friction angle. The reinforcement force distribution conserved the same shape for different friction angles.. This result is in agreement with the numerical study of Xie, and al., (2016) and the same from Chen (2017).

159 The Location of maximum reinforcement force is not influenced by the shear strength of the
160 soil. This result is in agreement with the numerical study of Tiwari and Samadhiya (2015) and
161 contradictory to some earlier researchers' (Shiwakoti et al, 1999) findings that the maximum
162 reinforcement force occurs at the bottom or mid-height of the slope.

163 **5. Conclusions**

164 This paper reports the results of numerical modeling of large-scale instrumented slope that
165 was constructed and monitored in a well-controlled environment. The numerically predicted
166 reinforcement forces and measured values provided an opportunity to compare numerical and
167 measured reinforcement. The results from the numerical models, the reinforcement force
168 distributions in the layers of the reinforced soil slopes were analyzed using limit analysis
169 iteratively and applying a Modified Bishop Method. Notable conclusions from this analysis
170 include:

171 - Location of maximum reinforcement force is not influenced by the shear strength of soil.
172 This contradicts with the observations of some earlier researchers that the maximum
173 reinforcement force occurs at bottom or mid-height of the slope.
174 - The soil internal friction angle effects reinforcement force distribution and the location of
175 maximum reinforcement force, this is in agreement with other numerical studies already
176 published.
177 - The target safety factor was a good indicator of the reinforcement forces values compared
178 to that measured in the reinforcements for geosynthetic-reinforced slopes built with
179 different configurations.
180 - Reinforcement force distribution is sensitive to values of soil-reinforcement interaction
181 coefficient. Using an appropriate interaction coefficient value can result in more accurate
182 estimates of mobilized reinforcement tensile force.

Numerical models tested and validated the process for determining the required reinforcement force distribution in each reinforcement layer proposed by Djeffal and Belkacemi (2020) against the full-scale slope. This process can be used to generate geosynthetic data for reinforced slope of greater heights, using different reinforcement types and arrangement, and other soils. These data can be used to fill gaps in the slope performance databases gathered from the limited number of slopes instrumented that are available in the literature.

Acknowledgements

This work is dedicated to the memory of Smain Belkacemi, our mentor, supervisor and teacher who inspired us and many other polytechnical engineers (1957–2020).

References

Allen, T. M., & Bathurst, R. J., 2019. Geosynthetic Reinforcement Stiffness Characterization for MSE Wall Design. Geosynthetics International, 26(6), 1-49.

Chen, J., Zhang, W., &Xue, J. (2017). Zoning of reinforcement forces in geosynthetic reinforced cohesionless soil slopes. Geosynthetics International, 24(6), 565–574.

Djeffal, H., &Belkacemi, S. (2020). Effect of soil-reinforcement interaction coefficient on reinforcement tension distribution of reinforced slopes. Geotextiles and Geomembranes, 48(4), 572–580.

Djeffal, H., &Belkacemi, S. (2021). A New Approach for Evaluating the Soil Slope Reinforcement Tensile Forces Using Limit Equilibrium Methods. Geotech Geol Eng 39, 2313–2327.

Miyata, Y., Bathurst, R.J. and Allen, T.M., 2018. Evaluation of tensile load model accuracy for PET strap MSE walls. Geosynthetics International. 25(6), 656-671.

206 Feng, S., Chen, J., Chen, H., Liu, X., Zhao, T., & Zhou, A., 2019. Analysis of sand-woven
207 geotextile interface shear behavior using DEM. Canadian Geotechnical Journal, 57(3), 433-
208 447.

209 Shukla, S., Sivakugan, N., & Das, B., 2009. Fundamental concepts of soil reinforcement -
210 an overview. International Journal of Geotechnical Engineering, 3(3), 329–342.

211 Mirzaalimohammadi, A., Ghazavi, M., Roustaei , M., Lajevardi, S.H., 2019. Pullout
212 response of strengthened geosynthetic interacting with fine sand. Geotextiles and
213 Geomembranes. 47(4), 530–541.

214 Salem, M. A., Hammad, M. A., & Amer, M. I., 2018. Field monitoring and numerical
215 modeling of 4.4 m-high mechanically stabilized earth wall. Geosynthetics International,
216 25(5), 1–45.

217 Shiwakoti DR, Pradhan TBS, Leshchinsky D (1999) Performance of geosynthetic-reinforced
218 soil structures at limit equilibrium state. Geosynth Int 5(6):555–587

219 Tiwari, G., &Samadhiya, N. K. (2015).Factors Influencing the Distribution of Peak Tension
220 in Geosynthetic Reinforced Soil Slopes. Indian Geotechnical Journal, 46(1), 34–44.

221 Xie, Y., Leshchinsky, B., & Yang, S. (2016). Evaluating reinforcement loading within
222 surcharged segmental block reinforced soil walls using a limit state framework. Geotextiles
223 and Geomembranes, 44(6), 832–844.

224 Yang, X. L., & Chen, J. H., 2019. Factor of Safety of Geosynthetic-Reinforced Slope in
225 Unsaturated Soils. International Journal of Geomechanics, 19(6), 04019041.

226 Zhang, F., Leshchinsky, D., Gao, Y., & Yang, S., 2018. Three-Dimensional Slope Stability
227 Analysis of Convex Turning Corners. Journal of Geotechnical and Geoenvironmental
228 Engineering, 144(6), 06018003.

229 Zornberg JG, Arriaga F (2003) Strain distribution within geosynthetic-reinforced slopes. J
230 Geotech GeoenvironEng 131(2):141–150

231 Zornberg, J.G., Sitar, N., Mitchell, J.K., 1998a. Performance of geosynthetic reinforced
232 slopes at failure. Journal of Geotechnical and Geoenvironmental Engineering, 124(8), 670–
233 683.

234

Figures

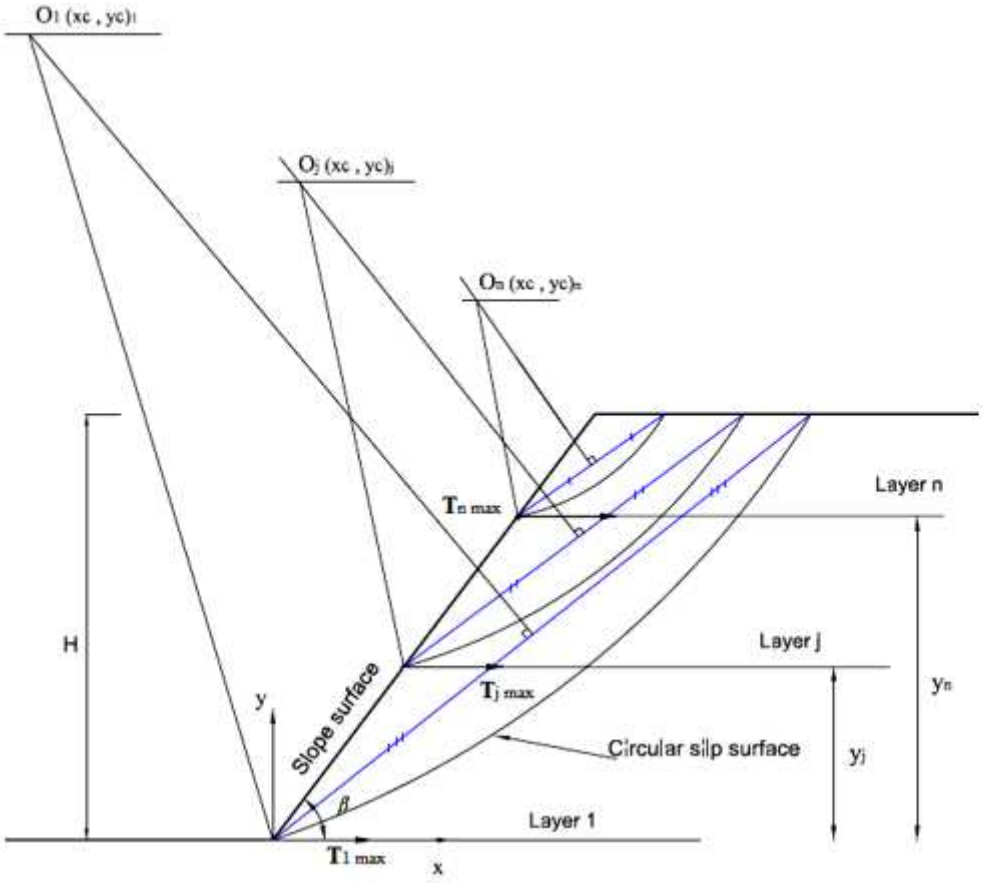

Figure 1

Modified Bishop's method-failure surfaces considered (Djeffal and Belkacemi, 2020)

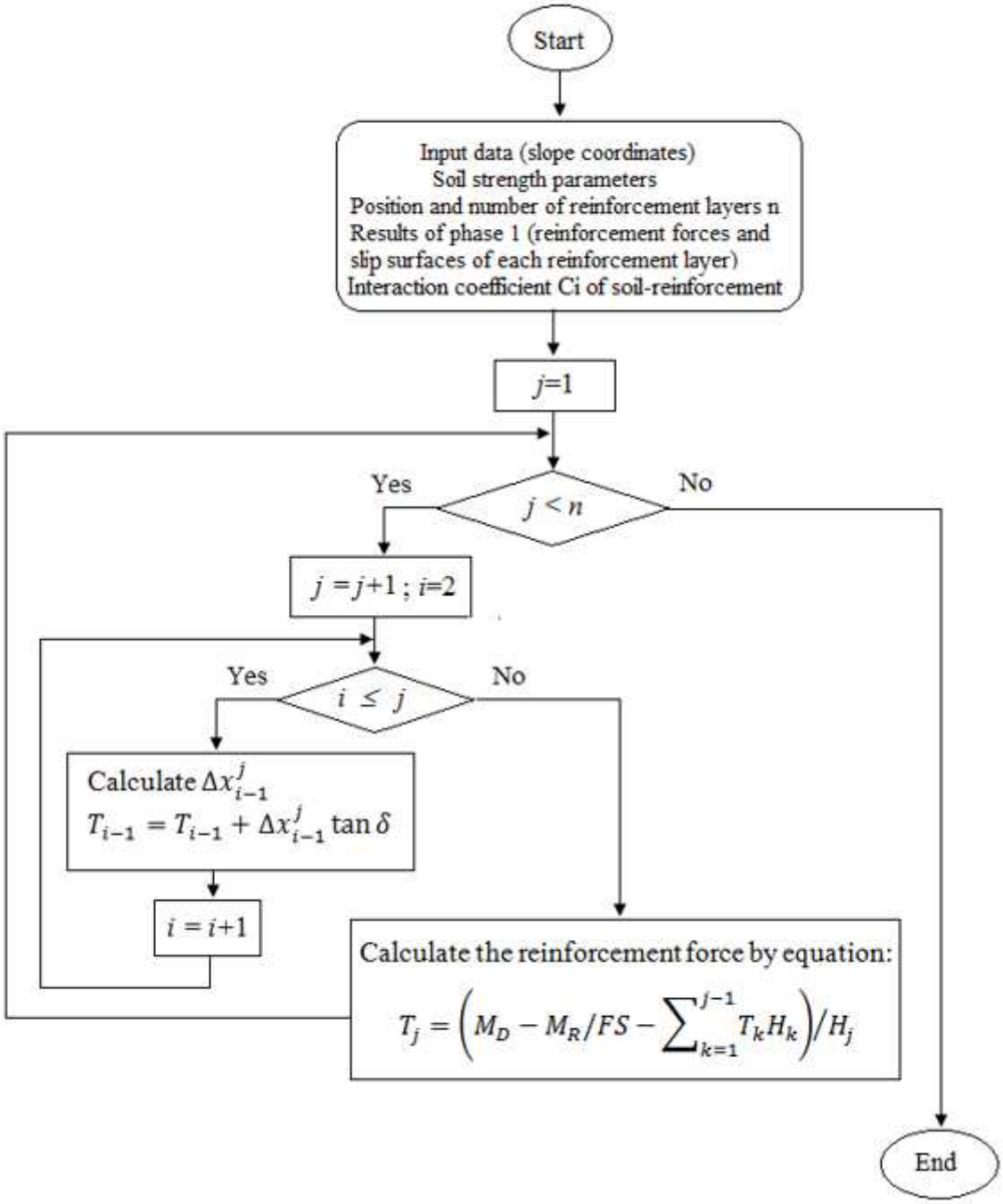

Figure 2

Flowchart to calculate the redistribution of the required tensile reinforcement forces (Djeffal and Belkacemi, 2020)

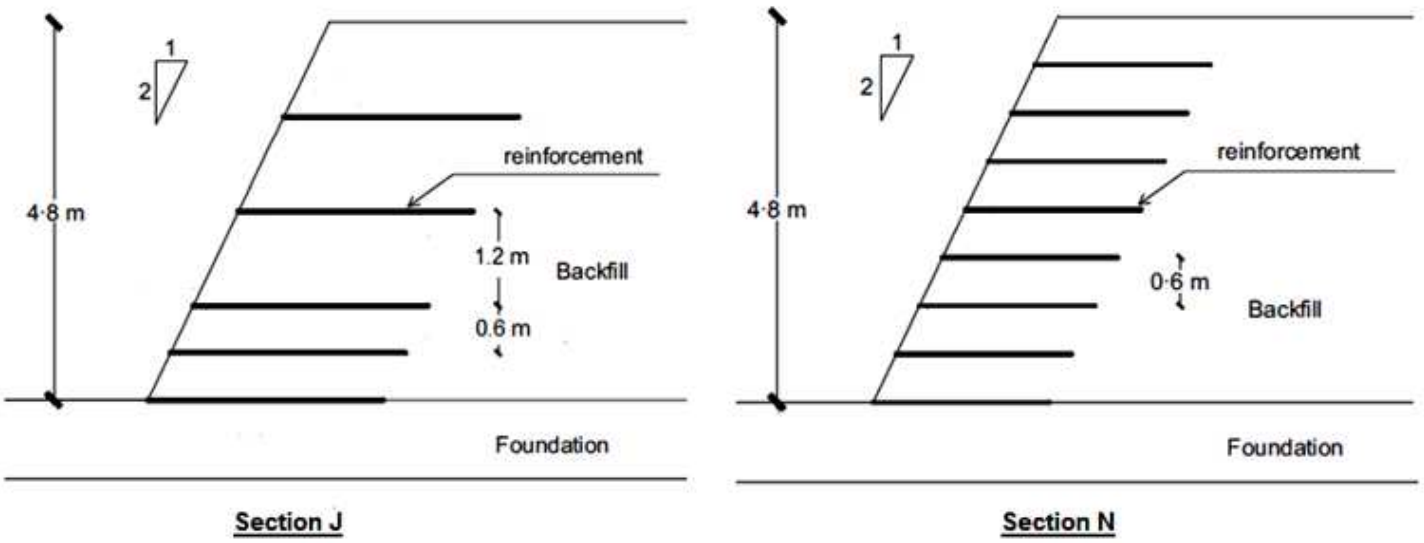

Figure 3

Numerical models of section J and section N (Fannin and Hermann 1990)

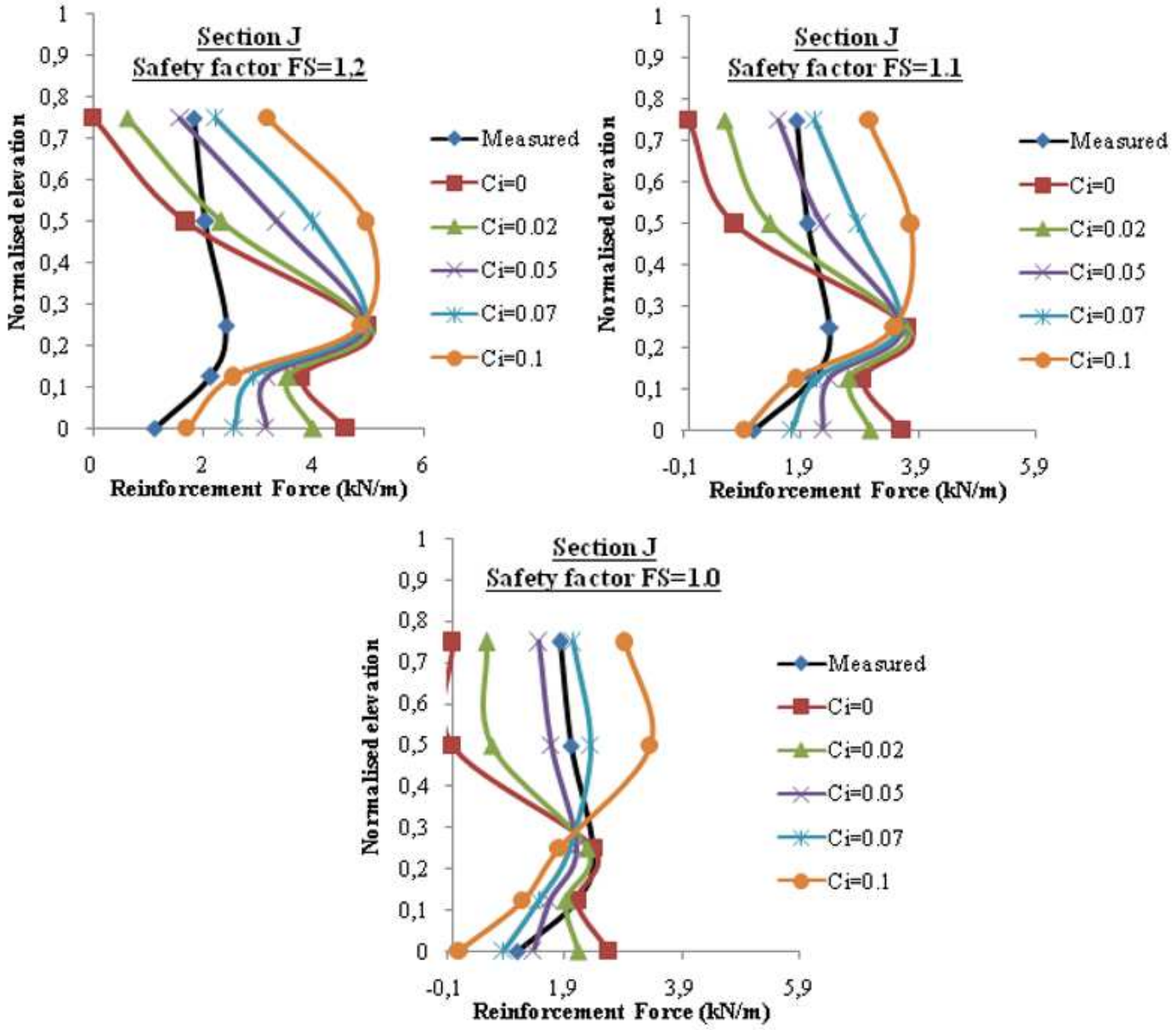

Figure 4

Reinforcement forces distribution as a function of the interaction coefficient- Section J

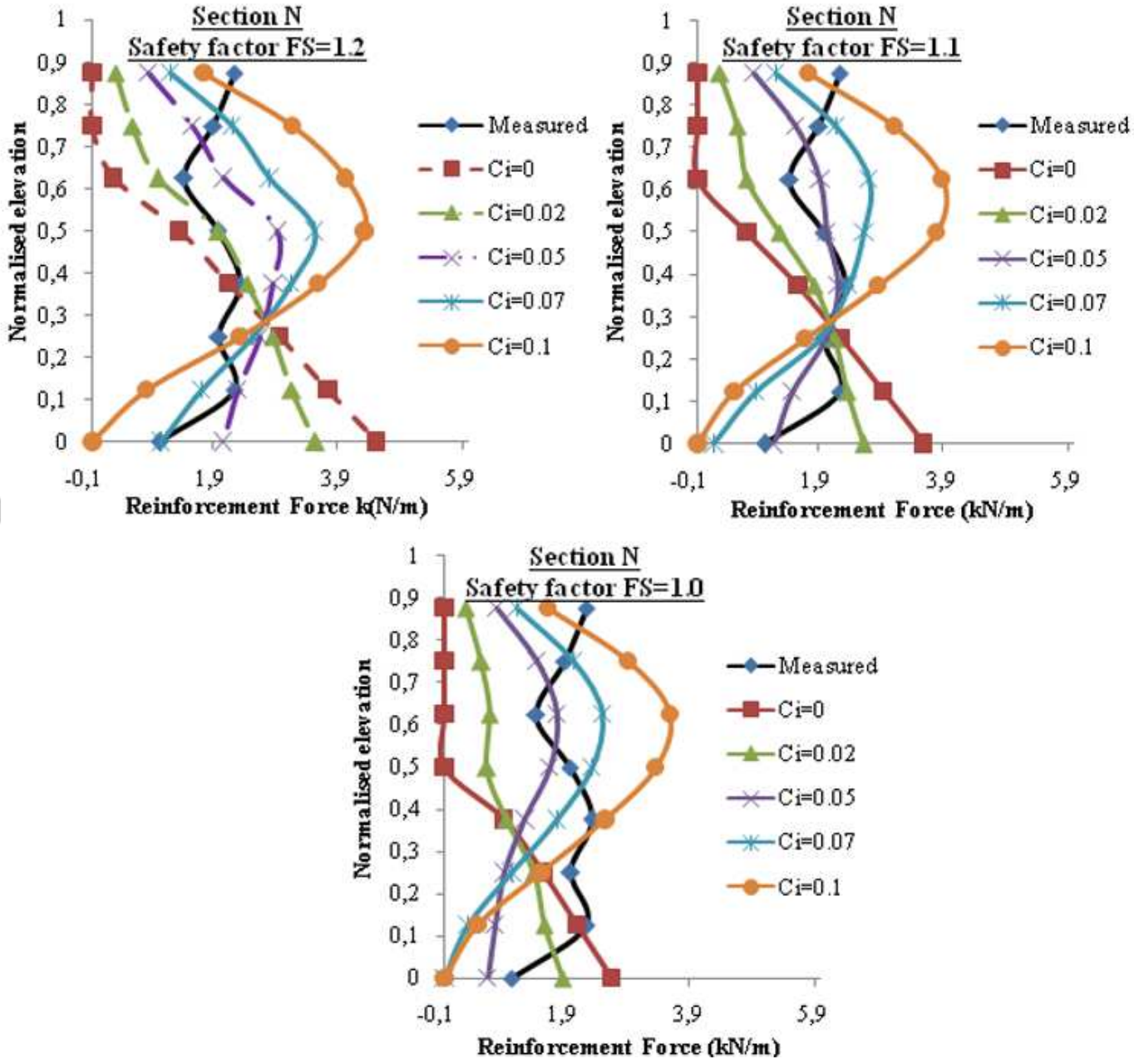

Figure 5

Reinforcement forces distribution as a function of the interaction coefficient- Section N

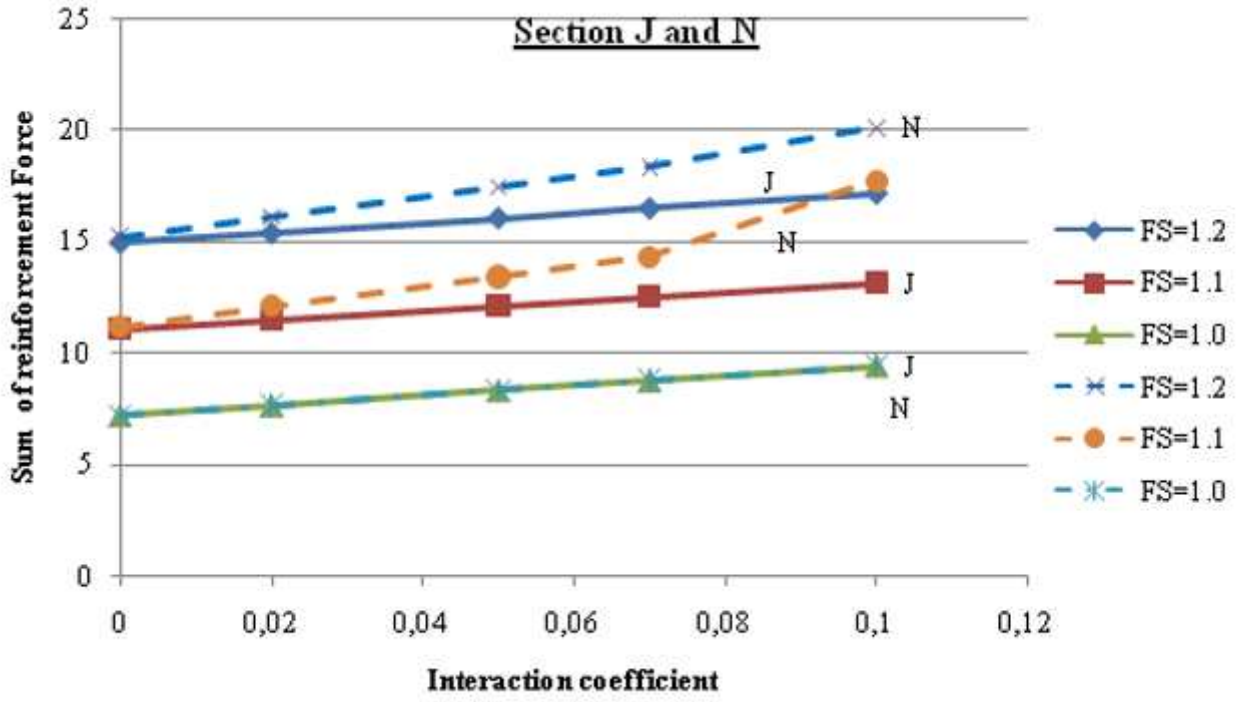

Figure 6

Sum of reinforcement force as a function of the interaction coefficient-Section J and N

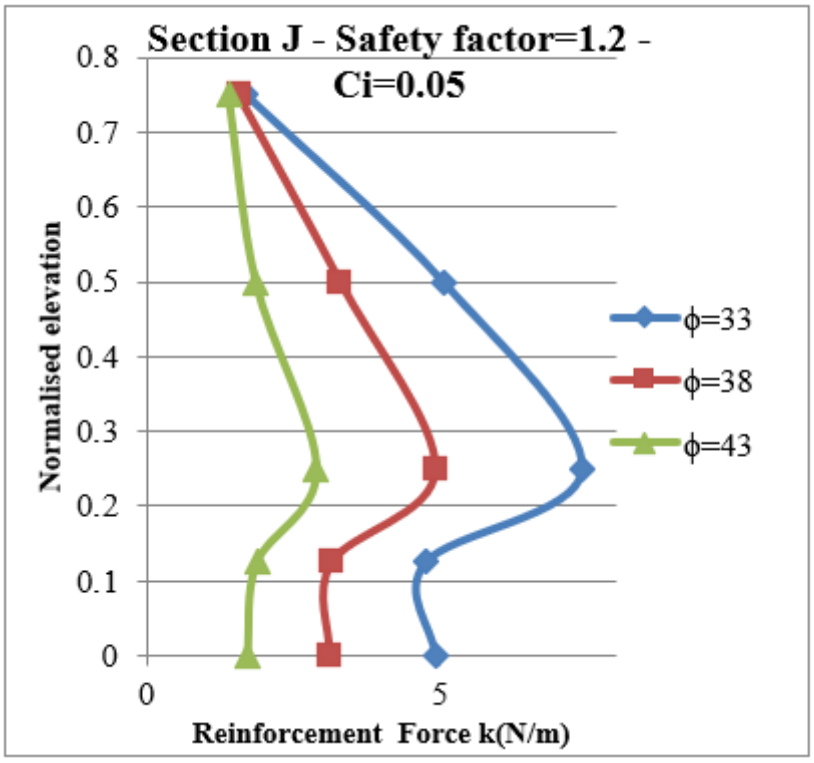

Figure 7

Variation of the required tensile reinforcement forces vs. height for different values of soil friction angle– Section J– Ci=0.05.

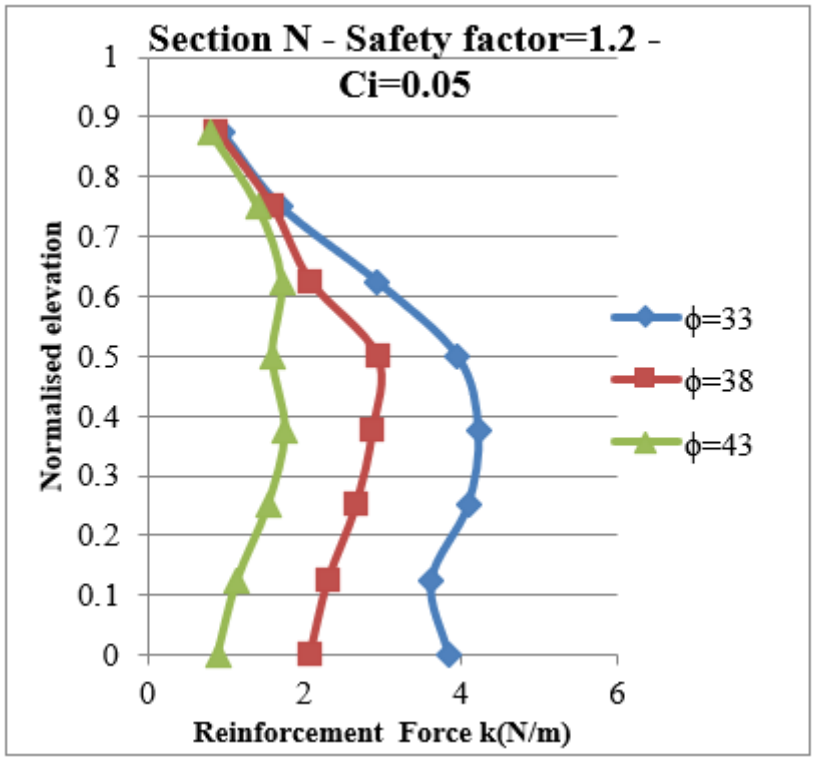

Figure 8

Variation of the required tensile reinforcement forces vs. height for different values of soil friction angle– Section N– Ci=0.05.